Published in final edited form as:
J Neurosurg. 2010 September ; 113(3): 656–665. doi:10.3171/2010.3.JNS091627.

WINCS-BASED WIRELESS ELECTROCHEMICAL MONITORING OF SEROTONIN (5-HT) USING FAST-SCAN CYCLIC VOLTAMMETRY: PROOF OF PRINCIPLE

Christoph J. Griessenauer, M.D.[1], **Su-Youne Chang, Ph.D.**[1], **Susannah J. Tye, Ph.D.**[1], **Christopher J. Kimble, M.A.**[2], **Kevin E. Bennet, B.S.Ch.E., M.B.A.**[2], **Paul A. Garris, Ph.D.**[3], and **Kendall H. Lee, M.D., Ph.D.**[1,4]

[1] Department of Neurosurgery, Mayo Clinic, Rochester, MN 55905

[2] Division of Engineering, Mayo Clinic, Rochester, MN 55905

[3] Department of Biological Sciences, Illinois State University, Normal, IL 61790

[4] Department of Physiology and Biomedical Engineering, Mayo Clinic, Rochester, MN 55905

Abstract

Object—We previously reported the development of a Wireless Instantaneous Neurotransmitter Concentration System (WINCS) for measuring dopamine and suggested that this technology may be useful for evaluating deep brain stimulation (DBS)-related neuromodulatory effects on neurotransmitter systems. WINCS supports fast-scan cyclic voltammetry (FSCV) at a carbon-fiber microelectrode (CFM) for real-time, spatially resolved neurotransmitter measurements. The FSCV parameters used to establish WINCS dopamine measurements are not suitable for serotonin, a neurotransmitter implicated in depression, because they lead to CFM fouling and a loss of sensitivity. Here, we incorporate into WINCS a previously described N-shaped waveform applied at a high scan rate to establish wireless serotonin monitoring.

Methods—FSCV optimized for the detection of serotonin consisted of an N-shaped waveform scanned linearly from a resting potential of, in V, +0.2 to +1.0, then to −0.1 and back to +0.2 at a rate of 1000 V/s. Proof of principle tests included flow injection analysis and electrically evoked serotonin release in the dorsal raphe nucleus of rat brain slices.

Results—Flow cell injection analysis demonstrated that the N waveform applied at a scan rate of 1000 V/s significantly reduced serotonin fouling of the CFM, relative to that observed with FSCV parameters for dopamine. In brain slices, WINCS reliably detected sub-second serotonin release in the dorsal raphe nucleus evoked by local high-frequency stimulation.

Conclusion—WINCS supported high-fidelity wireless serotonin monitoring by FSCV at a CFM. In the future such measurements of serotonin in large animal models and in humans may help to establish the mechanism of DBS for psychiatric disease.

CORRESPONDING AUTHOR INFORMATION: Kendall H. Lee, M.D., Ph.D., Department of Neurosurgery, Mayo Clinic, 200 First Street SW, Rochester, Minnesota 55905, Telephone: 507-284-2816; Fax: 507-284-5206, lee.kendall@mayo.edu.

Disclosure or Disclaimer: None

AUTHORS' CONTRIBUTION

Christoph J. Griessenauer performed the flow cell analysis and the assisted in the slice experiments, analyzed the data, made the figures, and wrote the manuscript. Su-Youne Chang performed the slice experiments and edited the manuscript. Susannah J. Tye co-wrote the manuscript. Christopher J. Kimble and Kevin E. Bennet were the engineers involved in WINCS hardware development. Paul A. Garris provided the expertise in fast-scan cyclic voltammetry, was involved in WINCS hardware development, and co-wrote the manuscript. Kendall H. Lee directed the research and co-wrote the manuscript.

Keywords

5-HT; Deep brain stimulation; Neuromodulation; Neurotransmitters; Serotonin; Voltammetry

INTRODUCTION

Major depressive disorder is associated with significant morbidity and mortality and is ranked as the second most disabling condition in the developed world [19], with lifetime prevalence in the United States of approximately 17% [43]. Serotonin (5-HT) is thought to play a key role in mediating the pathophysiologic mechanism of depression [44]. Indeed, selective 5-HT reuptake inhibitors (SSRIs) are a common effective pharmacotherapy for depression [60]. Recently, deep brain stimulation (DBS) has been shown to be an effective therapeutic option for treatment-resistant depression [39]. Whether modulation of 5-HT neurotransmission contributes to the anti-depressant effect of DBS, however, remains to be determined.

Fast-scan cyclic voltammetry (FSCV) at a carbon-fiber microelectrode (CFM) represents one measurement technique that may help to resolve this issue. FSCV supports rapid and chemically resolved monitoring at a microsensor [8,17,46]. Through repeated rapid application of a voltage scan, oxidative and reductive currents can be monitored at the sensing electrode surface to specifically identify the analyte. We have previously described the development of the Wireless Instantaneous Neurotransmitter Concentration System (WINCS) that supports FSCV for measurement of dopamine (DA) and have suggested that this technology may be useful for evaluating the neurotransmitter release hypothesis of DBS [7,50]. WINCS is a small, sterilizable battery-powered, wireless instrument designed in compliance with FDA-recognized consensus standards for medical electrical device safety. WINCS also demonstrated reduced susceptibility to ambient electrical noise and is therefore capable of performing high-fidelity electrochemical measurements outside of a faraday cage and in the noisy electromagnetic environment inside a typical operating room [7]. Thus, advantageous design features of WINCS will support FSCV measurements in large-animal models and assure patient safety by facilitating integration into the existing functional neurosurgical set-up.

We now expand the capability of WINCS to measure 5-HT with FSCV. At electrochemical parameters utilized for DA, the presence of 5-HT leads the formation of multiple 5-HT electrochemical byproducts [24]. These reactive byproducts accumulate at the CFM surface and cause rapid and irreversible fouling, thus significantly slowing response time and decreasing sensitivity over time. Several strategies are available to minimize these fouling processes [22, 28,52,56]. Jackson *et al.* described a distinct waveform to measure 5-HT *in vivo* [24], which we call here the '5-HT waveform'. Parameters for this N-shaped waveform are a resting potential of +0.2 (Volts) V and scans to +1.0 V, then to -0.1 V and back to +0.2 V and a scan rate of 1000 V/s. Using this waveform, WINCS was able to measure 5-HT with flow injection analysis as well as electrically evoked 5-HT release in the raphe nucleus of the rat brain slice with high-fidelity. The capability of WINCS to monitor 5-HT release with FSCV in large animal models and in the human operating room setting may help to define the mechanism of action of DBS for depression.

MATERIALS AND METHODS

Animals

Five adult male Sprague-Dawley rats, weighing 300 to 400 g, were used for brain slice testing. Rats were housed under standard conditions, with *ad libitum* access to food and water. Care was provided in accordance with NIH guidelines (publication 86–23) and approved by the Mayo Clinic Institutional Animal Care and Use Committee.

Wireless Instantaneous Neurotransmitter Concentration System (WINCS)

As we have previously reported, WINCS hardware incorporates circuitry that applies the FSCV waveform to the microsensor, in this case the CFM, samples the resulting sensor current, and transmits the current measurements to the WINCS base station via a Bluetooth radio link [2,7,50]. Data are displayed in several graphical formats, in nearly real time, by custom software (WINCSware) running on the base station.

FSCV at a CFM

For FSCV, two different waveform parameters were compared. Each was applied to the CFM every 100 ms (10 Hz). As described in the introduction, the so-called '5-HT waveform' consisted of a resting potential of +0.2 V scanned to +1.0 V, then to −0.1 V and back to +0.2 V that was applied at a rate of 1000 V/s [24]. The other waveform consisted of a resting potential in between scans of −0.4 V scanned to +1.0 V and back to −0.4 V and a scan rate of 300 V/s. We will refer to these parameters as the 'DA waveform'. These two waveforms are shown in Figure 1. As can be seen, the DA waveform (Figure 1A) is broader than the 5-HT waveform (Figure 1B). This is due to differences in scan rate and potential range. For example, the DA waveform, which has a duration of 9.3 ms, is applied at 300 V/s, whereas the 5-HT waveform, which lasts 2.2 ms, is applied at 1000 V/s. The DA waveform also covers a greater potential range than the 5-HT waveform (2.8 V versus 2.2 V, respectively).

The CFM was constructed by aspirating a single carbon fiber (r = 2.5 μm) (AmocoR T60) into a borosilicate glass capillary and pulling to a microscopic tip using a pipette puller (P-2000, Sutter Instruments, CA, USA). The exposed carbon fiber was trimmed to a final length of ~100 μm using a scalpel [10]. To exclude negatively charged interference, the tip of the CFM was dip coated with 5 % Nafion and dried under a heat gun three times [45]. The Ag/AgCl reference electrode was fabricated by chloridizing a 31 gauge silver wire [16].

Flow Injection Analysis

Flow injection analysis was used for *in vitro* measurements with FSCV at a CFM [33]. In this procedure, well established for device testing and microsensor calibration, a CFM is placed in a flowing stream of buffer and analyte is injected as a bolus. The buffer solution, composed of 150 mM sodium chloride and 12 mM Tris at a pH 7.4, was pumped across the CFM at a rate of 6 ml/min. An electronic loop injector, locally fabricated, introduced a bolus of analyte for 5 s into the flowing stream at defined test concentrations.

In vitro brain slice preparation

For the preparation of slices, 6- to 8-week-old male Sprague-Dawley rats were deeply anaesthetized with urethane (1.5 g/kg, i.p.; supplemented 15 min later with 0.5 g/kg, i.p.) and sacrificed by decapitation. The brain was rapidly removed and put into a chilled solution (5° C) in which NaCl was replaced with sucrose while the osmolarity was maintained at 307 mOsm [1]. Slices (400 μm thick) were cut in the coronal plane using a vibratome (Leica, Wetzlar, Germany). Slices were placed in an interface-style recording chamber (Fine Sciences Tools, Foster City, CA, USA), maintained at 35°C and allowed to recover for at least 2 h. The bathing medium contained (in mM): NaCl, 126; KCl, 2.5; $MgSO_4$, 1.2; NaH_2PO_4, 1.25; $CaCl_2$, 2.4; $NaHCO_3$, 26; HEPES, 20; D-glucose, 10. Medium was aerated with 95% O_2 and 5% CO_2 to a final pH of 7.4. For the first 20 min that slices were in the recording chamber, bathing medium contained an equal mixture of the normal NaCl and the sucrose-substituted solutions. Slices were perfused with drug for 20 min before postdrug data were collected.

Electrical Stimulation

A train of monophasic current pulses (200 μA, 2 ms duration) were delivered to a twisted bipolar stimulating electrode (Plastics One, MS 303/2, Roanoke, VA, USA) at a frequency of 60 Hz using an optical isolator and programmable pulse generator (Iso-Flex/Master-8; AMPI, Jerusalem, Israel) [37]. Stimulus trains, separated by > 5 min to assure sufficient time for 5-HT release to recovery, consisted of 10, 20 or 40 pulses.

Chemicals

Drugs were dissolved in distilled water at a stock concentration of 10 mM, diluted with flow injection analysis buffer or slice bathing medium to the final concentration. Fluoxetine hydrochloride, 5-HT hydrochloride and DA hydrochloride were purchased from Sigma (St. Louis, MO).

RESULTS

Comparison of the DA and 5-HT waveforms

In FSCV, scanning the potential at a high rate produces a large background current due to charging of the double layer capacitance of the exposed carbon fiber. Fortunately, this background current is stable over short times, so that it can be subtracted to reveal the considerably smaller faradaic currents generated by analyte electrochemistry. A plot of measured current as a function of applied potential is called a voltammogram. The background-subtracted voltammogram, which can be plotted individually or sequentially in a 3-D pseudo-color representation, serves as a chemical signature to identify the analyte detected during the measurement. Figures 2 and 3 show FSCV measurements of 5-HT collected by the aforementioned DA and 5-HT waveforms, respectively. Background currents plotted with voltage unfolded linearly are displayed in the bottom panel of Figures 2A and 3A. The top panel show the corresponding changes in applied voltage during the scan for each waveform and plotted with time. Note, for both waveforms, that the large background signal (black line) overshadows the smaller faradaic current for 5-HT (red line). Background subtraction plotted similarly, shown in the bottom panel of Figures 2B and 3B, reveals the 5-HT voltammogram. For reference, the voltage scan plotted versus time is also shown in the top panel.

Background-subtracted voltammograms collected by the two waveforms are clearly different. The voltammogram collected with the DA waveform, as shown in Figure 2B (bottom panel), exhibits an upward facing, oxidative peak and two downward facing, reductive peaks. The oxidation peak occurs at a potential of approximately +0.5 to 0.6 V, whereas the “double” reduction peaks correspond to potentials of 0 to −0.1 V and −0.4 to −0.5 V. A byproduct of 5-HT oxidation is responsible for the formation of this second reduction peak [24,29]. The deflection at 1.0 V is a switching artifact and unrelated to 5-HT electrochemistry. In contrast and shown in Figure 3B (bottom panel), only two peaks are evident in the background-subtracted voltammogram collected with the 5-HT waveform. The upward facing peak at approximately +0.6 to +0.7 V is due to oxidation of 5-HT to ρ-quinone-imine and the downward facing peak at 0 to −0.1 V is due to the reduction of the electroformed quinone back to 5-HT.

As shown in Figures 2C and 3C, all background-subtracted voltammograms collected during the recording are plotted sequentially in time using a pseudo-color display, with time as the x axis, voltage as the y axis, and current as the z or color axis. The brown color is zero current, established by background subtraction procedure. Color features, which occur between 5 and 10 s, represent 5-HT electrochemistry when the CFM is exposed to 5-HT during bolus ejection of flow injection analysis. The green-purple colors correspond to 5-HT oxidation, while the black-yellow colors correspond to 5-HT reduction. The vertical white line represents one voltammogram, as shown in Figures 2B and 3B, bottom panel.

The horizontal white line on the color plots, which is located at the peak oxidation potential for 5-HT, represents the change in 5-HT oxidative current with time. The resulting current change is shown in Figures 2D and 3D. Notice the faster dynamics of the measured bolus injection of 5-HT for the 5-HT waveform (Figure 3D) when compared to the DA (Figure 2D) waveform, as demonstrated by the sharper changes in current during the dynamic concentration change. The deflections around 5 and 10 s are injection artifacts. Comparison of DA and 5-HT waveform, as shown in Figures 2 and 3, was performed on four additional electrodes (data not shown).

To determine CFM fouling and loss of sensitivity to 5-HT, sequential injections of 5-HT were measured by the two waveforms as shown in Figure 4. Each point in Figure 4A represents maximal current collected at the peak oxidative potential for 5-HT and measured during a 10 μM injection of 5-HT. Data are the maximal signal expressed as a percent of the first injection. Buffer contained 1 μ5-HT to mimic the continuous exposure a CFM might encounter when implanted in the brain *in vivo*. In contrast to the 5-HT waveform, which produced a constant signal amplitude with each injection, there was a rapid decrease in sensitivity to 10 μM 5-HT with the DA waveform. In fact, by the 10^{th} injection, the 5-HT signal measured with the DA waveform decreased by approximately 50%. The background-subtracted voltammograms collected with either 5-HT (Figure 4B) or DA (Figure 4C) waveform demonstrated that the potentials at which 5-HT oxidative and reductive peaks occurred did not change with injection number. However, as expected, the amplitude of the oxidative peak for 5-HT decreased with the 10^{th} injection for the DA waveform, but only slightly for the 5-HT waveform. In these voltammograms, current is plotted with the voltage folded back onto itself. Similar observations were made on four different electrodes (data not shown).

Characterization of the 5-HT waveform

The 5-HT waveform was further characterized by determining concentration-response curves for 5-HT and DA, and comparing background-subtracted voltammograms for the different analytes. Concentration-response curves for 5-HT and DA and collected by the 5-HT waveform are compared in Figure 5. Figures 5A-D show representative pseudo-color plots of known 5-HT standard solutions (0.25, 2.5, 5 and 10 μM, respectively). Applying the same color range representing current to all four pseudo-color plots highlights the increase in oxidative current and reductive current with increasing 5-HT concentration. As in Figures 2D and 3D, the deflections towards the beginning and end of the bolus signal are an artifact of the loop injection and filtering, and unrelated to 5-HT electrochemistry. Figure 5E shows current measured at the peak oxidative potential for 5-HT (horizontal white lines on the pseudo-color plots 5A-D) during the bolus 5-HT injections and plotted with time. Note the increase in maximal current with increasing 5-HT concentration. Figure 5F plots maximal current with analyte concentration. While there was a linear increase in current with concentration for both 5-HT ($r^2 = 0.95$) and DA ($r^2 = 0.99$), the 5-HT waveform was approximately 20-times more sensitive to 5-HT than to DA. All measurements were collected at the same CFM. Similar concentration-response curves were also recorded at four additional CFMs (data not shown).

Several analytes, including changes in pH, can be considered “interferents” to the voltammetric measurement of 5-HT in the brain, because all would contribute to current monitored at the peak oxidation potential for 5-HT if present. Figure 6 shows background-subtracted voltammograms, collected with the 5-HT waveform, for 5-HT (A, 10 μM), DA (B, 10 μM), alkaline (C, pH = 8.5), and acidic (D, pH = 6.5) solutions. Based on several characteristics, voltammograms for DA and pH can readily be distinguished from 5-HT. For example, the oxidation peak of DA is shifted to the right (more positive) and broader than that for 5-HT, and the reductive peak appears on the negative excursion for 5-HT, but not for DA. Moreover,

acidic and alkaline pH changes produce voltammograms with peaks of different shapes and appearing at different voltages compared to 5-HT.

Brain slice 5-HT recording with the 5-HT waveform

As shown in Figure 7, the *in vitro* slice preparation of the dorsal raphe nucleus was used to demonstrate the capability of WINCS to detect 5-HT in brain tissue. Panel 7A shows the experimental setup, with WINCS in the foreground and the slice chamber and microelectrode manipulators in the background. A concentric bipolar stimulating electrode and a CFM were placed in the dorsal raphe nucleus approximately 100 μm apart, as shown in a schematic drawing in Panel 7B. A representative pseudo-color plot in Panel 7C shows sequential voltammograms indicative of 5-HT release in the slice during a 40-pulse train delivered at 7 s. Current traces recorded at the peak oxidative potential for 5-HT are shown in Panel 7D. Note the increase in signal amplitude with increasing number of stimulus pulses. Return of the evoked signal to baseline levels after maximal 5-HT release represents cellular reuptake of 5-HT. Oxidative and reductive peaks in the background-subtracted voltammogram (INSET, see vertical dashed lines) match those expected for 5-HT. As shown in Panel 7E, bath application of 5 μM fluoxetine, a SSRI, delays the signal return to baseline after a 20 pulse stimulation, indicative of slowed 5-HT reuptake. Electrically evoked 5-HT was recorded in four additional slices and showed similar results (data not shown).

DISCUSSION

We previously demonstrated that WINCS is able to measure DA, adenosine and glutamate [2,7,50]. Here, we expand the chemical repertoire of WINCS to include 5-HT, a neurotransmitter strongly implicated in depression. Compatible with the operating room setting and designed for human use, WINCS supports FSCV at a CFM for chemically, temporally and spatially resolved neurotransmitter monitoring. By wirelessly measuring 5-HT with high-fidelity, WINCS is well suited for testing, both in large animal models and in humans, the hypothesis that DBS for depression may modulate 5-HT systems.

WINCS

WINCS is a small, sterilizable, battery-powered, wireless device designed in compliance with FDA-recognized consensus standards for medical electrical device safety. With important safety issues addressed, particularly those related to line-powered devices, WINCS is compatible with chemical measurements in humans. Analog-to-digital conversion of the recorded signal near the point of acquisition, combined with digital telemetry, enhances signal quality and provides enhanced immunity to electromagnetic interference. This capability for WINCS to support chemical measurements outside the faraday cage, which is typically required by conventional hardwired devices to block ambient noise, makes this device functional in an operating room setting [2,7]. WINCS can also transmit data to a remotely located base station, so, coupled with its small size, it does not contribute to crowding in the busy operating room area. Collectively, these characteristics allow the application of WINCS for clinical as well as research purposes, such as in large animal models.

FSCV for 5-HT

FSCV measurements of 5-HT at a CFM are challenging [24,25,29]. With a waveform used for DA measurements [20], here the so-called DA waveform, 5-HT concentration dynamics assessed by a bolus injection were slowed (Fig. 2D) and sensitivity to 5-HT decreased over time (Fig. 4A). These measurement limitations, due to the formation of reactive byproducts that foul the surface of the CFM, are overcome with careful selection of different FSCV parameters [9,22,24,28]. Indeed, the use of FSCV parameters identified by Jackson *et al.* [24], here the so-called 5-HT waveform, greatly accelerated observed 5-HT dynamics (Fig. 3D) and permitted the

measurement of repetitive 5-HT injections with only slight decrement in signal amplitude (Fig. 4A). Moreover, the 5-HT waveform was highly sensitive to 5-HT (Fig. 5) and permitted high-fidelity monitoring of 5-HT in brain tissue (Fig. 7). Taken together, these data establish real-time, wireless 5-HT monitoring with WINCS.

By expanding its repertoire to include 5-HT, WINCS can now take full advantage of the analytical attributes of FSCV at a CFM for monitoring this neurotransmitter important for neuropsychiatric diseases. For example, the microsensor can be positioned in the raphe nucleus of the rat (Fig. 7B) for spatially selective neurotransmitter monitoring in this small brain region. The high temporal resolution of FSCV permits direct observation of the dynamic change elicited by fluoxetine on neuronal 5-HT reuptake (Fig. 7E), an action thought to underlie the mechanism of SSRI action for treating depression [60]. Finally, the chemical resolution of FSCV is well suited for distinguishing 5-HT from putative interferents (Fig. 6).

5-HT and depression

These proof of principle measurements demonstrating the capabilities of WINCS to reliably measure 5-HT might be relevant for future research on the role of 5-HT in a variety of neuronal processes and diseases, including depression. Serotoninergic projections from the raphe nuclei provide prominent innervations to neuronal circuitries processing emotions [21,41]. 5-HT transporters and receptors have been autoradiographically localized in regions belonging to the limbic cortico-striato-pallido-thalamic circuits [58]. Cortical elements of this circuitry are the medial orbitofrontal cortex, the anterior cingulate including the subgenual cingulate cortex (Cg25) and the agranular insular cortex. Subcortical connections running in the anterior internal capsule target the nuclei caudatus and accumbens. Via the globus pallidus, the dorsal substantia nigra and the ventral tegmental area connectivity to the dorsomedial thalamic nucleus is established. Projections back to the cortices via the anterior internal capsule and the inferior thalamic peduncle complete the circuit [30].

In depression, a 5-HT imbalance is generally discussed as an underlying pathophysiologic mechanism [13]. Serotonin enhancing drugs like SSRIs and tricyclic antidepressants are a common effective pharmacotherapy for depression [60]. People carrying the short allele of the 5-HT transporter (5HTT), a gene that affects the promoter region encoding for 5HTT, have an increased vulnerability of developing depression. However, the clinical implications of these findings and causative relationship remain to be determined [11]. In clinical studies with patients recovering from depression, tryptophan depletion led to a relapse; however, healthy controls did not experience mood changes [51,61]. Tryptophan depletion is a technique employed to lower plasma and brain tryptophan by administering an amino acid mixture free of the 5-HT precursor tryptophan [13]. A recent single photon emission computed tomography study (SPECT) in healthy, euthymic male individuals demonstrated that positive and negative changes in subjective happiness associated with rapid tryptophan depletion were significantly correlated with changes in the regional cerebral blood flow in the subgenual cingulate cortex (Cg25) and associated regions [53]. Taken together, the 5-HT system and its inherent interaction with other neurotransmitter networks are likely to play a role in mediating depression.

DBS and Depression

Although the clinical efficacy of DBS is well established, the biological mechanisms of action still remain to be elucidated. Compared to ablative lesioning surgery, DBS is characterized as being relatively less-invasive, focused, reversible and modulatory [19]. Proposed mechanisms of action include silencing of stimulated neurons, modulation of network activity and neurotransmission and long-term synaptic plasticity [18,38]. High-frequency stimulation is also thought to induce excitation of efferent axons that results in release of neurotransmitters from remote efferent terminals [40,42]. Release of neurochemicals may contribute to the beneficial

effect of DBS in a variety of diseases including tremor [5], Parkinson's disease [34–36] and possibly depression.

Depression and other significant psychiatric side effects have been reported to be highly comorbid in Parkinson's disease patients receiving DBS of the subthalamic nucleus (STN) [4,12,14,15,23,32,47,55]. On the other hand, mood improvement after DBS of the internal globus pallidus for tardive dyskinesia in a patient suffering from major depression has been observed [31]. A recent study of bilateral STN-DBS in a rat model of Parkinson's disease resulted in decreased firing of serotoninergic neurons in the dorsal raphe nucleus as well as induction of depression like behavior, suggesting modulatory effects of DBS on the 5-HT system [54]. Thus, neuropsychiatric consequences of DBS for movement disorders are currently receiving much needed scientific attention.

Moreover, based on the successful application of DBS as a treatment for movement disorders [6], several therapeutic trials have recently been conducted to investigate DBS as a treatment for various psychiatric diseases including treatment resistant depression. Case reports and small series reports on the efficacy of DBS as a therapy for treatment-resistant depression are promising, though preliminary [3,26,27,31,39,49,57,59]. Potential DBS targets for treatment resistant depression identified in the literature include white matter adjacent to Cg25 [27,39], ventral striatum/nucleus accumbens [3,57], inferior thalamic peduncle [26,59], rostral cingulate cortex (area 24a) [19] and lateral habenula [19,48]. Thus far, DBS electrodes have only been implanted in the first three of these structures [19]. The ventral striatum/NAc, the Cg25 and the inferior thalamic peduncle are important components of the limbic cortico-striatal-pallido-thalamocortical loop. Given that DBS in treatment of depression may include neuromodulation of the serotoninergic system, our current demonstration of the capability of WINCS to reliably measure 5-HT might be helpful in clarifying this exciting question.

Future directions

Now that WINCS for 5-HT detection is available, future work will be directed toward elucidation of potential 5-HT modulation by DBS. We expect that WINCS-based 5-HT measurements may ultimately be an asset to DBS research and may provide chemical feedback regarding the efficacy of the targeted site for neuromodulation. For example, chemical signals collected by WINCS at an implanted microsensor could serve as a feedback signal for localizing DBS electrode placement and adjusting stimulation parameters. Future studies based on this proof of principle work will be directed toward *in vivo* 5-HT measurements in brain regions related to DBS in animal models, and potentially, in humans.

Conclusion

Here we have demonstrated that WINCS effectively monitors 5-HT in brain tissue. We conclude that this capability of WINCS may be helpful in testing the hypothesis that effectiveness of DBS for depression is at least partially related to modulation of the 5-HT system.

Acknowledgments

The authors would like to acknowledge the contribution of the engineers of Division of Engineering of Mayo Clinic, April E. Horne, David M. Johnson, Kenneth R. Kressin, Justin C. Robinson, Sidney V. Whitlock and Bruce A. Winter for their invaluable efforts in the realization of the WINCS device and software.

Financial and Material Support: This work was supported by: NIH (K08 NS 52232 award to KHL), Mayo Foundation (2008–2010 Research Early Career Development Award for Clinician Scientists award to KHL), Mathews Foundation (John T. and Lillian Mathews Professorship in Neuroscience award), Austrian Academy of Sciences (DOC-fellowship to CJG), and American Australian Association (Sir Keith Murdoch Fellowship award to SJT).

Abbreviations

5-HT	5-Hydroxytryptamine (Serotonin)
5-HTT	5-HT transporter
Aq	Aqueduct
CFM	Carbon Fiber Microelectrode
Cg25	Brodmann Area 25 of the subgenual cingulated cortex
DA	Dopamine
DBS	Deep brain stimulation
DR	dorsal raphe
FDA	Food and Drug Administration
FSCV	Fast-scan cyclic voltammetry
MDD	Major depressive disorder
NAc	Nucleus accumbens
SSRI	Selective serotonin reuptake inhibitor
STN	Subthalamic nucleus
V	Volts
WINCS	Wireless Instantaneous Neurotransmitter Concentration System

References

1. Aghajanian GK, Rasmussen K. Intracellular studies in the facial nucleus illustrating a simple new method for obtaining viable motoneurons in adult rat brain slices. Synapse 1989;3:331–338. [PubMed: 2740992]
2. Agnesi F, Tye SJ, Bledsoe JM, Griessenauer CJ, Kimble CJ, Sieck GC, et al. Wireless Instantaneous Neurotransmitter Concentration System-based amperometric detection of dopamine, adenosine, and glutamate for intraoperative neurochemical monitoring. J Neurosurg 2009;111:701–711. [PubMed: 19425899]
3. Aouizerate B, Cuny E, Martin-Guehl C, Guehl D, Amieva H, Benazzouz A, et al. Deep brain stimulation of the ventral caudate nucleus in the treatment of obsessive-compulsive disorder and major depression. Case report. J Neurosurg 2004;101:682–686. [PubMed: 15481726]
4. Bejjani BP, Damier P, Arnulf I, Thivard L, Bonnet AM, Dormont D, et al. Transient acute depression induced by high-frequency deep-brain stimulation. N Engl J Med 1999;340:1476–1480. [PubMed: 10320386]
5. Bekar L, Libionka W, Tian GF, Xu Q, Torres A, Wang X, et al. Adenosine is crucial for deep brain stimulation-mediated attenuation of tremor. Nat Med 2008;14:75–80. [PubMed: 18157140]
6. Benabid AL, Chabardes S, Mitrofanis J, Pollak P. Deep brain stimulation of the subthalamic nucleus for the treatment of Parkinson's disease. Lancet Neurol 2009;8:67–81. [PubMed: 19081516]
7. Bledsoe JM, Kimble CJ, Covey DP, Blaha CD, Agnesi F, Mohseni P, et al. Development of the Wireless Instantaneous Neurotransmitter Concentration System for intraoperative neurochemical monitoring using fast-scan cyclic voltammetry. J Neurosurg 2009;111:712–723. [PubMed: 19425890]
8. Borland, LM.; Michael, AC. An introduction to electrochemical methods in neuroscience. In: Michael, AC.; Borland, LM., editors. Electrochemical Methods for Neuroscience. Boca Raton: CRC Press; 2007. p. 1-15.
9. Bunin MA, Prioleau C, Mailman RB, Wightman RM. Release and uptake rates of 5-hydroxytryptamine in the dorsal raphe and substantia nigra reticulata of the rat brain. J Neurochem 1998;70:1077–1087. [PubMed: 9489728]

10. Cahill PS, Walker QD, Finnegan JM, Mickelson GE, Travis ER, Wightman RM. Microelectrodes for the measurement of catecholamines in biological systems. Anal Chem 1996;68:3180–3186. [PubMed: 8797378]
11. Caspi A, Sugden K, Moffitt TE, Taylor A, Craig IW, Harrington H, et al. Influence of life stress on depression. moderation by a polymorphism in the 5-HTT gene. Science 2003;301:386–389. [PubMed: 12869766]
12. Castelli L, Perozzo P, Genesia ML, Torre E, Pesare M, Cinquepalmi A, et al. Sexual well being in parkinsonian patients after deep brain stimulation of the subthalamic nucleus. J Neurol Neurosurg Psychiatry 2004;75:1260–1264. [PubMed: 15314111]
13. Cowen PJ. Serotonin and depression. pathophysiological mechanism or marketing myth? Trends Pharmacol Sci 2008;29:433–436. [PubMed: 18585794]
14. Doshi P, Bhargava P. Hypersexuality following subthalamic nucleus stimulation for Parkinson's disease. Neurol India 2008;56:474–476. [PubMed: 19127045]
15. Doshi PK, Chhaya N, Bhatt MH. Depression leading to attempted suicide after bilateral subthalamic nucleus stimulation for Parkinson's disease. Mov Disord 2002;17:1084–1085. [PubMed: 12360564]
16. Garris PA, Christensen JR, Rebec GV, Wightman RM. Real-time measurement of electrically evoked extracellular dopamine in the striatum of freely moving rats. J Neurochem 1997;68:152–161. [PubMed: 8978721]
17. Garris, PA.; Greco, GP.; Sandberg, SG.; Pongmayteegul, GHS.; Heidenreich, BA., et al. In vivo voltammetry with telemetry. In: Michael, AC.; Borland, LM., editors. Electrochemical Methods for Neuroscience. Boca Rhaton; CRC Press: 2007. p. 233-259.
18. Hammond C, Ammari R, Bioulac B, Garcia L. Latest view on the mechanism of action of deep brain stimulation. Mov Disord 2008;23:2111–2121. [PubMed: 18785230]
19. Hauptman JS, DeSalles AA, Espinoza R, Sedrak M, Ishida W. Potential surgical targets for deep brain stimulation in treatment-resistant depression. Neurosurg Focus 2008;25:E3. [PubMed: 18590380]
20. Heien ML, Johnson MA, Wightman RM. Resolving neurotransmitters detected by fast-scan cyclic voltammetry. Anal Chem 2004;76:5697–5704. [PubMed: 15456288]
21. Hensler JG. Serotonergic modulation of the limbic system. Neurosci Biobehav Rev 2006;30:203–214. [PubMed: 16157378]
22. Hentall ID, Pinzon A, Noga BR. Spatial and temporal patterns of serotonin release in the rat's lumbar spinal cord following electrical stimulation of the nucleus raphe magnus. Neuroscience 2006;142:893–903. [PubMed: 16890366]
23. Houeto JL, Mesnage V, Mallet L, Pillon B, Gargiulo M, du Moncel ST, et al. Behavioural disorders, Parkinson's disease and subthalamic stimulation. J Neurol Neurosurg Psychiatry 2002;72:701–707. [PubMed: 12023409]
24. Jackson BP, Dietz SM, Wightman RM. Fast-scan cyclic voltammetry of 5-hydroxytryptamine. Anal Chem 1995;67:1115–1120. [PubMed: 7717525]
25. Jackson BP, Wightman RM. Dynamics of 5-hydroxytryptamine released from dopamine neurons in the caudate putamen of the rat. Brain Res 1995;674:163–166. [PubMed: 7773688]
26. Jimenez F, Velasco F, Salin-Pascual R, Hernandez JA, Velasco M, Criales JL, et al. A patient with a resistant major depression disorder treated with deep brain stimulation in the inferior thalamic peduncle. Neurosurgery 2005;57:585–593. discussion 585–593. [PubMed: 16145540]
27. Johansen-Berg H, Gutman DA, Behrens TE, Matthews PM, Rushworth MF, Katz E, et al. Anatomical connectivity of the subgenual cingulate region targeted with deep brain stimulation for treatment-resistant depression. Cereb Cortex 2008;18:1374–1383. [PubMed: 17928332]
28. John CE, Budygin EA, Mateo Y, Jones SR. Neurochemical characterization of the release and uptake of dopamine in ventral tegmental area and serotonin in substantia nigra of the mouse. J Neurochem 2006;96:267–282. [PubMed: 16300629]
29. John, CE.; Jones, SR. Fast Scan Cyclic Voltammetry of Dopamine and Serotonin in Mouse Brain Slices. In: Michael, AC.; Borland, LM., editors. Electrochemical Methods for Neuroscience. Boca Rhaton: CRC Press; 2007. p. 49-62.
30. Kopell BH, Greenberg BD. Anatomy and physiology of the basal ganglia. implications for DBS in psychiatry. Neurosci Biobehav Rev 2008;32:408–422. [PubMed: 17854894]

31. Kosel M, Sturm V, Frick C, Lenartz D, Zeidler G, Brodesser D, et al. Mood improvement after deep brain stimulation of the internal globus pallidus for tardive dyskinesia in a patient suffering from major depression. J Psychiatr Res 2007;41:801–803. [PubMed: 16962613]
32. Krack P, Batir A, Van Blercom N, Chabardes S, Fraix V, Ardouin C, et al. Five-year follow-up of bilateral stimulation of the subthalamic nucleus in advanced Parkinson's disease. N Engl J Med 2003;349:1925–1934. [PubMed: 14614167]
33. Kristensen EW, Wilson RM, Wightman RM. Dispersion in flow injection analysis measured with microvoltammetric electrodes. Anal Chem 1986;58:986–988.
34. Lee KH, Blaha CD, Garris PA, Mohseni P, Horne AE, Bennet KE, et al. Evolution of Deep Brain Stimulation. Human Electrometer and Smart Devices Supporting the Next Generation of Therapy. Neuromodulation: Technology at the Neural Interface. in press.
35. Lee KH, Blaha CD, Harris BT, Cooper S, Hitti FL, Leiter JC, et al. Dopamine efflux in the rat striatum evoked by electrical stimulation of the subthalamic nucleus. potential mechanism of action in Parkinson's disease. Eur J Neurosci 2006;23:1005–1014. [PubMed: 16519665]
36. Lee KH, Chang SY, Roberts DW, Kim U. Neurotransmitter release from high-frequency stimulation of the subthalamic nucleus. J Neurosurg 2004;101:511–517. [PubMed: 15352610]
37. Lowry CA, Hale MW, Evans AK, Heerkens J, Staub DR, Gasser PJ, et al. Serotonergic systems, anxiety, and affective disorder. focus on the dorsomedial part of the dorsal raphe nucleus. Ann N Y Acad Sci 2008;1148:86–94. [PubMed: 19120094]
38. Lujan JL, Chaturvedi A, McIntyre CC. Tracking the mechanisms of deep brain stimulation for neuropsychiatric disorders. Front Biosci 2008;13:5892–5904. [PubMed: 18508630]
39. Mayberg HS, Lozano AM, Voon V, McNeely HE, Seminowicz D, Hamani C, et al. Deep brain stimulation for treatment-resistant depression. Neuron 2005;45:651–660. [PubMed: 15748841]
40. McIntyre CC, Mori S, Sherman DL, Thakor NV, Vitek JL. Electric field and stimulating influence generated by deep brain stimulation of the subthalamic nucleus. Clin Neurophysiol 2004;115:589–595. [PubMed: 15036055]
41. Michelsen KA, Schmitz C, Steinbusch HW. The dorsal raphe nucleus--from silver stainings to a role in depression. Brain Res Rev 2007;55:329–342. [PubMed: 17316819]
42. Miocinovic S, Parent M, Butson CR, Hahn PJ, Russo GS, Vitek JL, et al. Computational analysis of subthalamic nucleus and lenticular fasciculus activation during therapeutic deep brain stimulation. J Neurophysiol 2006;96:1569–1580. [PubMed: 16738214]
43. Murray CJ, Lopez AD. Alternative projections of mortality and disability by cause 1990–2020. Global Burden of Disease Study. Lancet 1997;349:1498–1504. [PubMed: 9167458]
44. Nichols DE, Nichols CD. Serotonin receptors. Chem Rev 2008;108:1614–1641. [PubMed: 18476671]
45. Pennington JM, Millar J, CPLJ, Owesson CA, McLaughlin DP, Stamford JA. Simultaneous real-time amperometric measurement of catecholamines and serotonin at carbon fibre 'dident' microelectrodes. J Neurosci Methods 2004;140:5–13. [PubMed: 15589328]
46. Robinson DL, Hermans A, Seipel AT, Wightman RM. Monitoring rapid chemical communication in the brain. Chem Rev 2008;108:2554–2584. [PubMed: 18576692]
47. Romito LM, Raja M, Daniele A, Contarino MF, Bentivoglio AR, Barbier A, et al. Transient mania with hypersexuality after surgery for high frequency stimulation of the subthalamic nucleus in Parkinson's disease. Mov Disord 2002;17:1371–1374. [PubMed: 12465087]
48. Sartorius A, Henn FA. Deep brain stimulation of the lateral habenula in treatment resistant major depression. Med Hypotheses 2007;69:1305–1308. [PubMed: 17498883]
49. Schlaepfer TE, Cohen MX, Frick C, Kosel M, Brodesser D, Axmacher N, et al. Deep brain stimulation to reward circuitry alleviates anhedonia in refractory major depression. Neuropsychopharmacology 2008;33:368–377. [PubMed: 17429407]
50. Shon YM, Chang SY, Tye SJ, Kimble CJ, Bennet KE, Blaha CD, et al. Comonitoring of adenosine and dopamine using the Wireless Instantaneous Neurotransmitter Concentration System. proof of principle. J Neurosurg 2010;112:539–548. [PubMed: 19731995]
51. Smith KA, Fairburn CG, Cowen PJ. Relapse of depression after rapid depletion of tryptophan. Lancet 1997;349:915–919. [PubMed: 9093253]
52. Swamy BE, Venton BJ. Carbon nanotube-modified microelectrodes for simultaneous detection of dopamine and serotonin in vivo. Analyst 2007;132:876–884. [PubMed: 17710262]

53. Talbot PS, Cooper SJ. Anterior cingulate and subgenual prefrontal blood flow changes following tryptophan depletion in healthy males. Neuropsychopharmacology 2006;31:1757–1767. [PubMed: 16407892]
54. Temel Y, Boothman LJ, Blokland A, Magill PJ, Steinbusch HW, Visser-Vandewalle V, et al. Inhibition of 5-HT neuron activity and induction of depressive-like behavior by high-frequency stimulation of the subthalamic nucleus. Proc Natl Acad Sci U S A 2007;104:17087–17092. [PubMed: 17942692]
55. Temel Y, Kessels A, Tan S, Topdag A, Boon P, Visser-Vandewalle V. Behavioural changes after bilateral subthalamic stimulation in advanced Parkinson disease. a systematic review. Parkinsonism Relat Disord 2006;12:265–272. [PubMed: 16621661]
56. Threlfell S, Exley R, Cragg SJ, Greenfield SA. Constitutive histamine H2 receptor activity regulates serotonin release in the substantia nigra. J Neurochem 2008;107:745–755. [PubMed: 18761715]
57. van Kuyck K, Gabriels L, Cosyns P, Arckens L, Sturm V, Rasmussen S, et al. Behavioural and physiological effects of electrical stimulation in the nucleus accumbens. a review. Acta Neurochir Suppl 2007;97:375–391. [PubMed: 17691326]
58. Varnas K, Halldin C, Hall H. Autoradiographic distribution of serotonin transporters and receptor subtypes in human brain. Hum Brain Mapp 2004;22:246–260. [PubMed: 15195291]
59. Velasco M, Velasco F, Jimenez F, Carrillo-Ruiz JD, Velasco AL, Salin-Pascual R. Electrocortical and behavioral responses elicited by acute electrical stimulation of inferior thalamic peduncle and nucleus reticularis thalami in a patient with major depression disorder. Clin Neurophysiol 2006;117:320–327. [PubMed: 16403484]
60. Willis-Owen SA, Turri MG, Munafo MR, Surtees PG, Wainwright NW, Brixey RD, et al. The serotonin transporter length polymorphism, neuroticism, and depression. a comprehensive assessment of association. Biol Psychiatry 2005;58:451–456. [PubMed: 16023085]
61. Young SN, Smith SE, Pihl RO, Ervin FR. Tryptophan depletion causes a rapid lowering of mood in normal males. Psychopharmacology (Berl) 1985;87:173–177. [PubMed: 3931142]

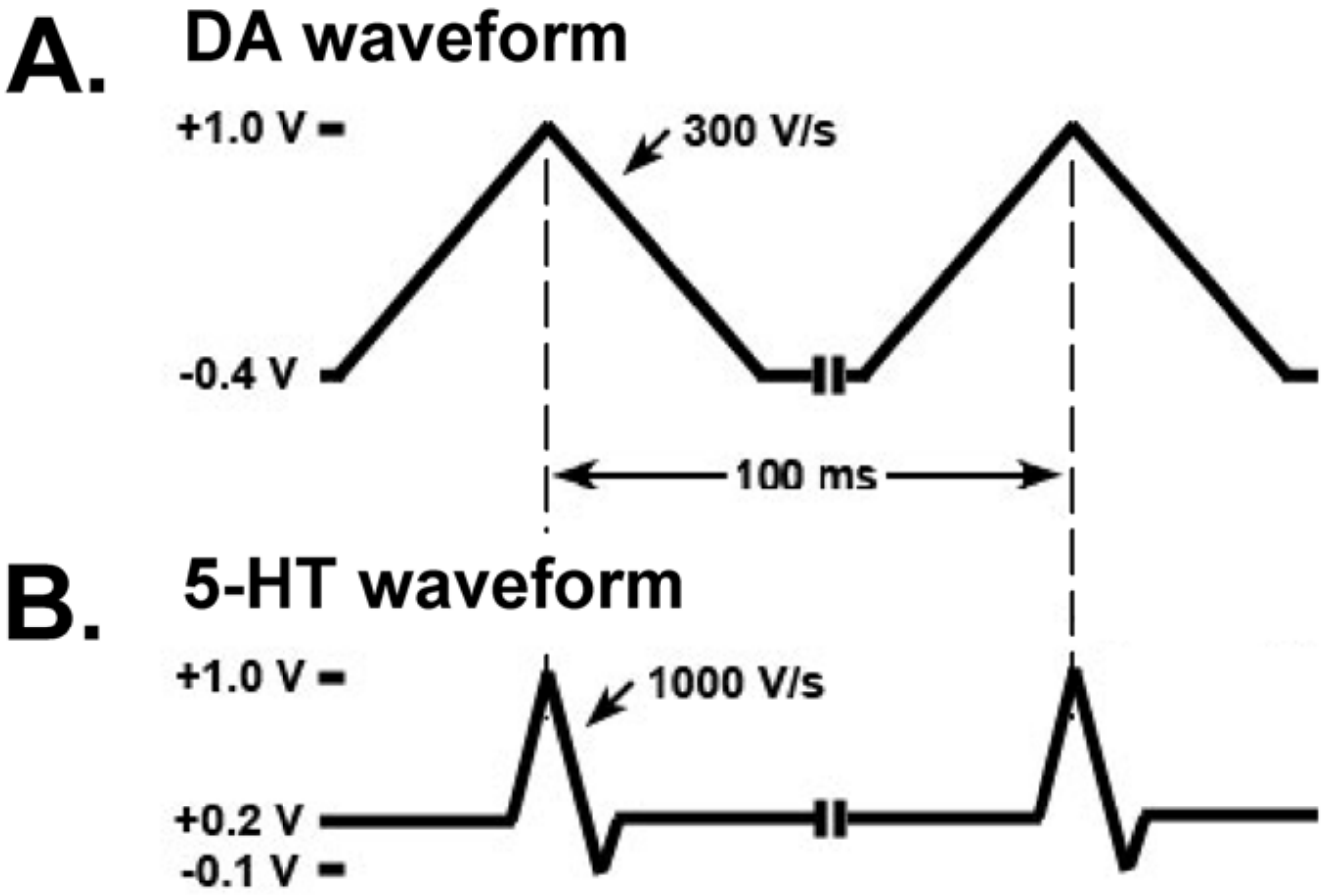

Figure 1. FSCV waveform comparison

A. DA waveform consisting of a resting potential of −0.4 V scanned to +1.0 V and back to −0.4 V and a scan rate of 300 V/s. **B.** 5-HT waveform consisting of a resting potential of +0.2 V scanned to +1.0 V, then to −0.1 V and back to +0.2 V and a scan rate of 1000 V/s.

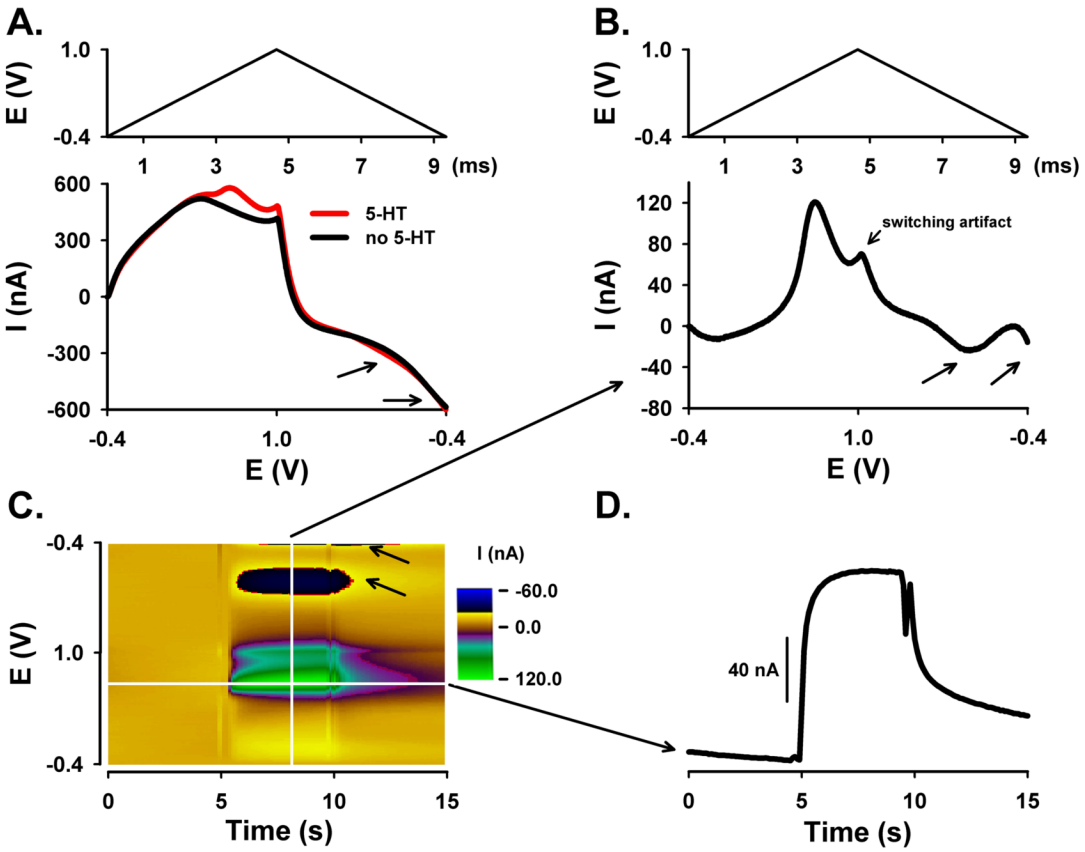

Figure 2. DA waveform for the detection of 5-HT using flow injection analysis

A. Background current with (red) and without (black) 5-HT plotted with voltage unfolded linearly (bottom panel) with DA waveform (top panel). **B.** Background-subtracted linear (unfolded) voltammogram (arrows identify the two reduction peaks) (bottom panel) with DA waveform (top panel). **C.** Pseudo-color plot (10 μM 5-HT). **D.** Current measured at the peak oxidative potential for 5-HT during the bolus injection and plotted with time.

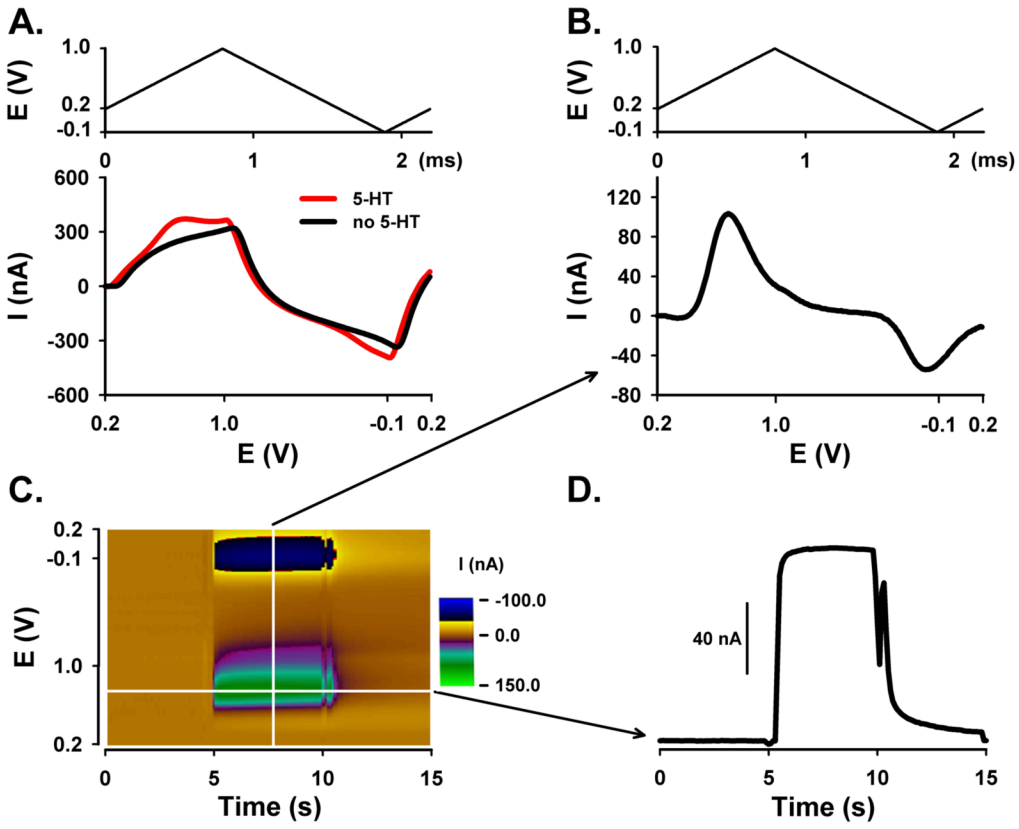

Figure 3. 5-HT waveform for the detection of 5-HT using flow injection analysis

A. Background current with (red) and without (black) 5-HT plotted with voltage unfolded linearly (bottom panel) with 5-HT waveform (top panel). **B.** Background-subtracted linear (unfolded) voltammogram (bottom panel) with 5-HT waveform (top panel). **C.** Pseudo-color plot (10 μM 5-HT). **D.** Current measured at the peak oxidative potential for 5-HT during the bolus injection and plotted with time.

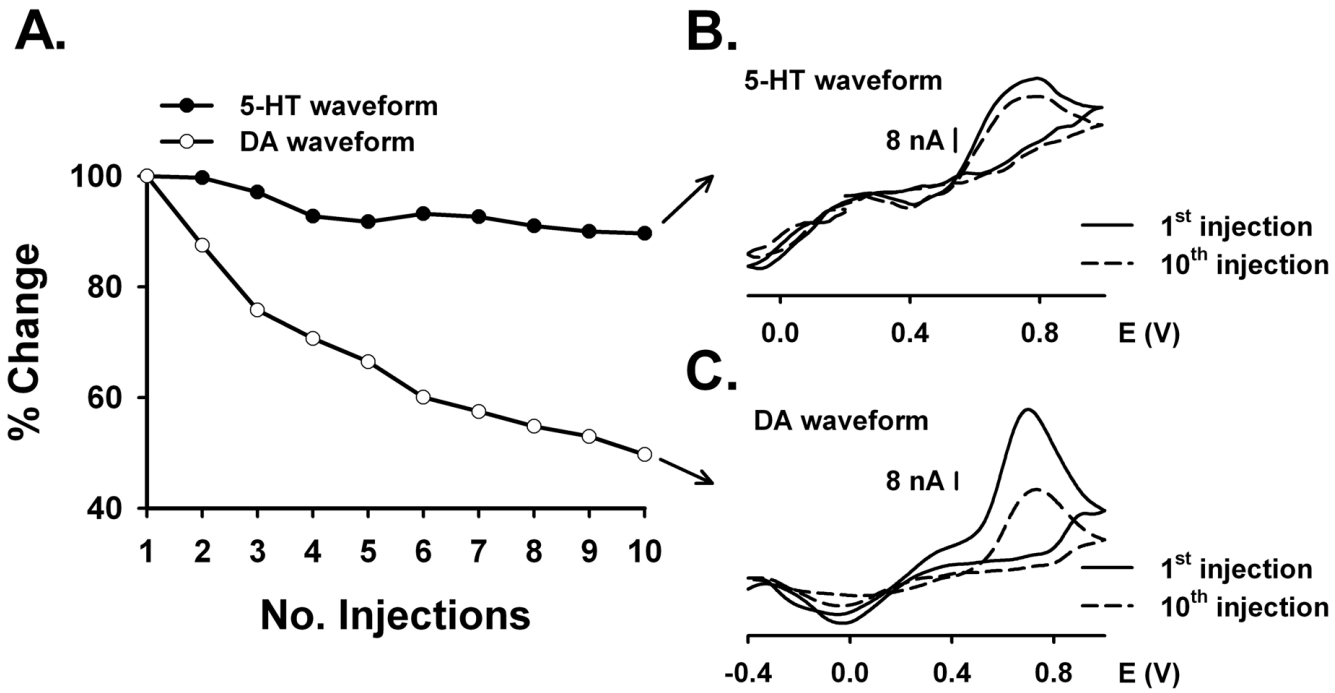

Figure 4. Comparison of the effects of DA and 5-HT waveforms on sequential injections of 10 μM 5-HT

A. Sensitivity change in % within 10 consecutive 5-HT injections. **B.** Serotonin waveform: background-subtracted voltammograms comparing 1st (solid line) and 10th injection (dashed line). **C.** Dopamine waveform: background-subtracted voltammograms comparing 1st (solid line) and 10th injection (dashed line).

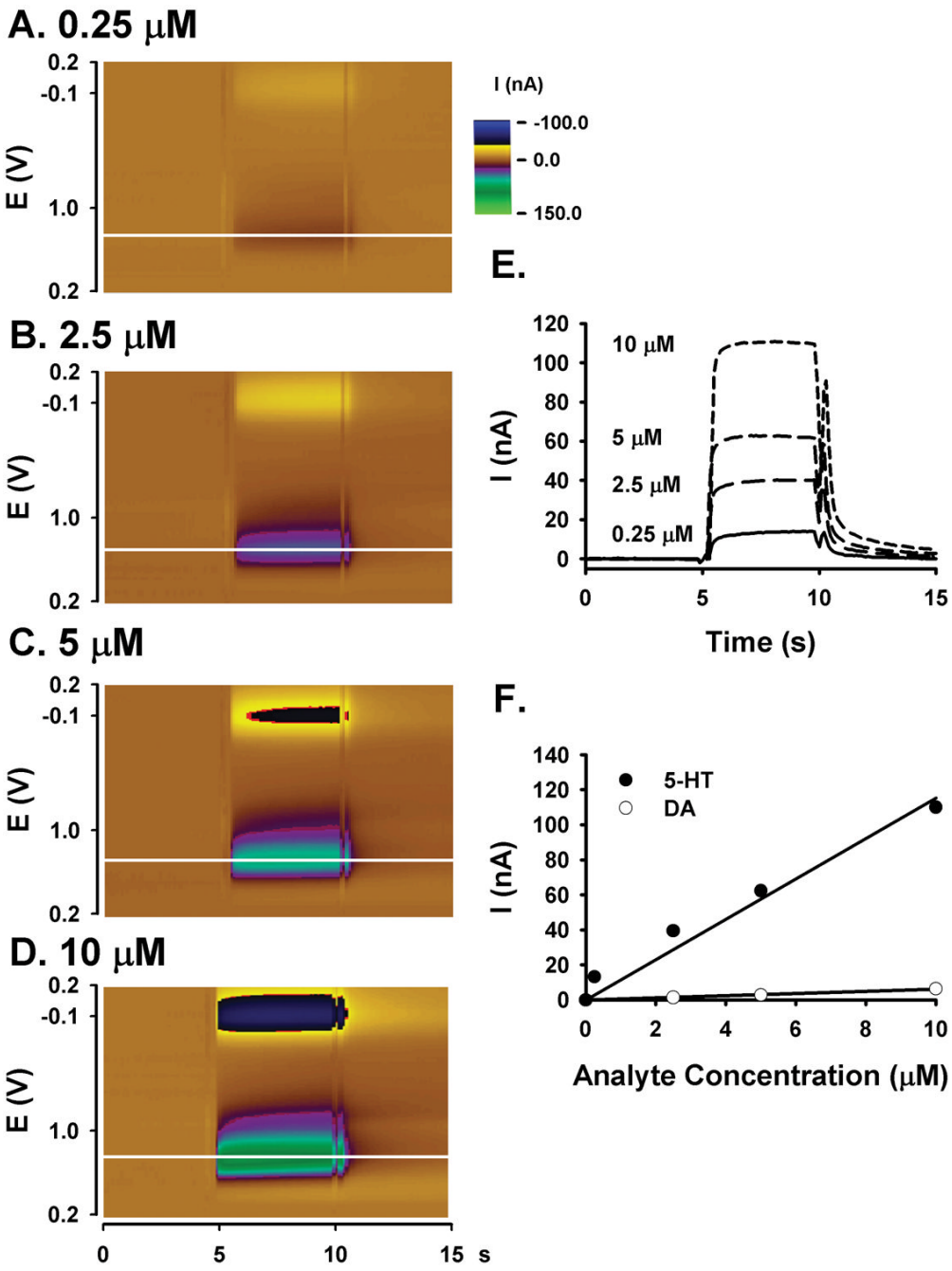

Figure 5. 5-HT and DA calibration curves collected with the 5-HT waveform

A. - D. Pseudo-color plot (0.25, 2.5, 5, 10 μM 5-HT). **E.** Current measured at the peak oxidative potential (horizontal white line on the pseudo-color plots) for a bolus injection of 5-HT. Increasing current corresponds to increasing 5-HT concentration (0.25, 2.5, 5, 10 μM 5-HT). **F.** 5-HT (closed circles) and DA (open circles) calibration curves. The solid line is the best linear fit.

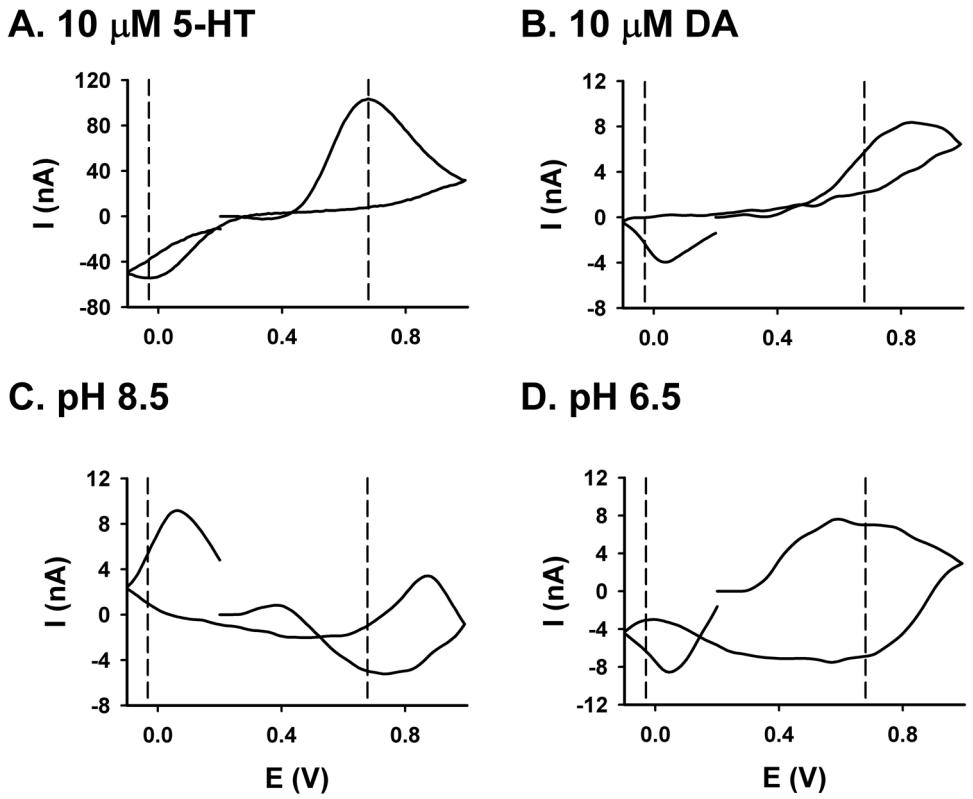

Figure 6. Comparison of background-subtracted cyclic voltammograms for different analytes
A. 10 μM 5-HT. **B.** 10 μM DA **C.** Alkaline pH change (from 7.4 to 8.5). **D.** Acidic pH change (from 7.4 to 6.5).

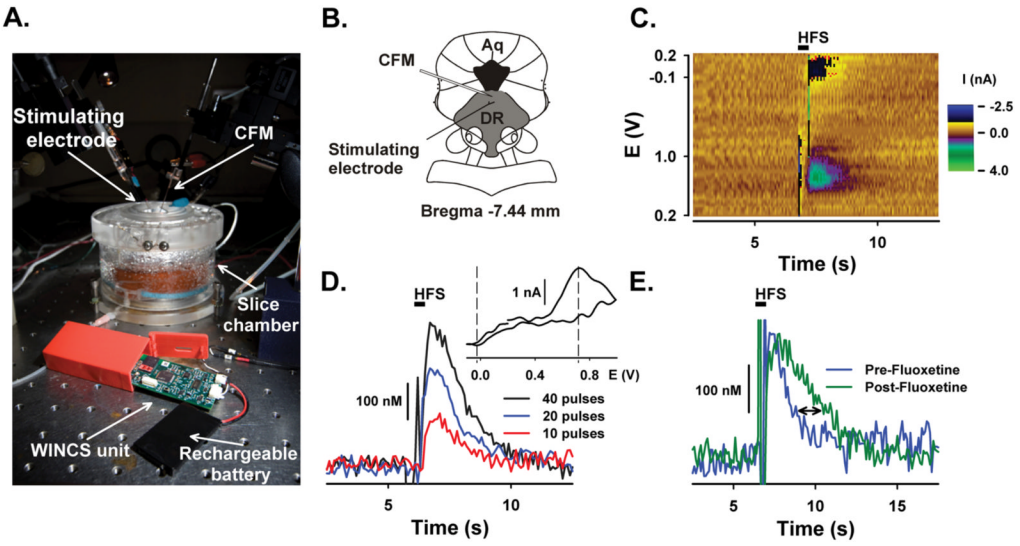

Figure 7. Detection of 5-HT in the dorsal raphe nucleus slice

A. Photograph of the slice chamber, WINCS unit with rechargeable battery, stimulating electrode and CFM. **B.** Cartoon drawing showing the position of the CFM and stimulating electrode in the brain slice (DR: dorsal raphe, Aq: Aqueduct). **C.** Pseudo-color plot for electrically evoked 5-HT (40 pulses). Black bar indicates time of stimulation (HFS: High-frequency stimulation). **D.** Electrically evoked 5-HT levels elicited by trains of 10, 20 and 40 pulses. INSET: Background-subtracted voltammogram for a 40-pulse train. **E.** Electrically evoked 5-HT levels before and after the application of 5 μM fluoxetine (20 pulses). Stimulation pulses (200 μA, 2 ms duration) were applied at a 60 Hz frequency.